

## Alignment of Digitized Whole-Mount Histopathology Slides to Prostate MR Images

S. M. Noworolski<sup>1,2</sup>, R. F. Guo<sup>3</sup>, G. D. Reed<sup>1</sup>, K. Kuchinsky<sup>4</sup>, K. Greene<sup>5</sup>, P. Carroll<sup>5</sup>, D. B. Vigneron<sup>1,2</sup>, J. Kurhanewicz<sup>1,2</sup>, and J. Simko<sup>4</sup>

<sup>1</sup>Radiology and Biomedical Imaging, University of California, San Francisco, San Francisco, CA, United States, <sup>2</sup>Graduate Group in Bioengineering, University of California, San Francisco & Berkeley, San Francisco & Berkeley, CA, United States, <sup>3</sup>Electrical Engineering, University of California, Berkeley, Berkeley, CA, United States, <sup>4</sup>Pathology, University of California, San Francisco, San Francisco, CA, United States, <sup>5</sup>Urology, University of California, San Francisco, San Francisco, CA, United States

### Introduction

Step-section histopathology of the excised prostate is the gold standard for distinguishing cancer and other abnormal tissues. To determine the accuracy of MR imaging for identifying prostate cancer and for discriminating among the Gleason Grades of cancer, accurate correlation to pathology is required. To date, most correlative studies have been performed with the prostate sectioned into quarters, each undergoing distortion and shrinkage, leading to limited correlations. Even with recent whole-mount histopathology slides of the prostate, alignments have been performed visually or on geometric divisions of the prostate (ie. sextant based analyses). This limits the assessment of MR. Both a more accurate alignment of pathology to MRI and an assessment of its limitations is required. In this study, digitized whole mount histopathology slides were semi-automatically aligned to prostate MR images. The quality of alignment was assessed for two groups: 1) in which the prostate was molded to imitate the MR shape prior to fixing during pathological analysis and 2) in which the prostate was not molded.

### Methods

Ten untreated patients scheduled for prostatectomy were scanned on a GE 3T scanner with a FSE sequence (TR/effective TE=6000/100ms), FOV=140, 3mm slices. T2-weighted MR images were acquired as part of a 3T prostate MR exam. Five of the patients had their prostate molded by securing the excised gland into a plastic mesh basket before fixation. This basket was made in-house of heat sensitive moldable plastic and was designed such that the rectal surface of the prostate underwent a concave curvature, designed to imitate the inflated endorectal probe. Additionally, a cover was secured to the anterior portion of the prostate to create a slight compression of the prostate, as the endorectal probe typically produces a 15% compression in the anterior/posterior direction [Kim 2005].

The prostate was manually segmented on the T2-weighted images (Fig 1E). Prostatectomy specimens were formalin-fixed (with or without molding), then serially cross-sectioned at 4-5mm intervals and entirely embedded in paraffin, and then cut as whole-mount histologic sections and digitized. In-house software written in C and Image Magick (ImageMagick Studio LLC) were used to modify the images. The digitized histopathology images were automatically cropped into slices (Fig 1A) and labels and extraneous markings removed (Fig 1B). Any remaining markings were manually removed, if required. Matching slides and a correspondence rate were visually determined. Histopathology slides were automatically centered and rotated to align with the corresponding MR images (Fig 1B). Next, the pathology slides were aligned in two ways: 1) with only a global stretching/shrinking, and 2) with a line-by-line stretching/ shrinking. The second approach stretched/shrank the rows horizontally to match the MRI prostate size (Fig 1C) and then stretched/ shrank the vertical columns to match the MRI prostate (Fig 1D). The % overlap was calculated and compared in the two approaches. Three visually identified landmarks marking the boundary of the peripheral zone and the central gland were compared on an aligned midgland pathology slide and MR slice for all cases. Distances between corresponding landmarks were measured and compared in 2D, as z-correspondence was visually selected.

### Results

Figure 1 shows the alignment steps and the morphed pathology slide (Fig 1D) to correspond to the T2-weighted MRI (Fig 1E). The red arrow points to the cancer. The morphed pathology slide has greater overlap with the MR prostate image than the original pathology slide.

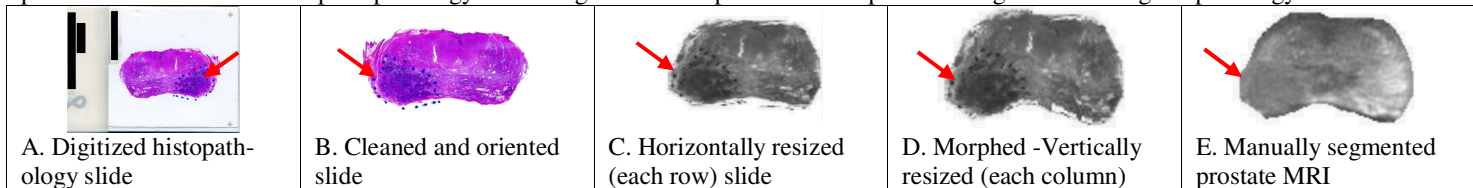


**Figure 1** – Steps for aligning histopathology to MRI, showing correspondence of the morphed histopathology slide to the MRI.

For the rigid body alignment with only global stretching/ shrinking, there was relatively poor overlap, which varied greatly across the slices (see Table 1). After employing the line-by-line stretching/shrinking algorithm, the %overlap was significantly improved in all cases. Visual assessments of the alignments showed good agreement, with landmark distances =  $2.5 \pm 1.5$  mm, but ranging up to 8mm. The molded cases tended to have shorter average and maximum landmark distances, but this did not reach significance. In one case, a central gland BPH nodule appeared to have shifted to a different axial slice of the prostate relative to the matching peripheral zone tissue. This case did not have the prostate molded when fixed during pathological processing.

### Discussion

The study demonstrated that rigid-only alignment of whole-mount histopathology slides to MR images did not yield a high degree of overlap. Computationally morphing the prostate allowed an almost complete overlap between the pathology slides and the MR images with good alignment of internal structures. Molding the prostate during pathological preparation of the gland may provide a better alignment of internal structures within the prostate, but this did not reach significance in this small population. Additionally, this study demonstrated that tissue distortion can be quite marked, necessitating assurance of alignment beyond % overlap before using the aligned pathology to classify MR tissue types.

**References** 1. Kim Y, et al. Med Phys. 32(12): 3569-3578. 2005. **Acknowledgments:** ACS: MRSG-0508701-CCE , NIH: CA079980, CA111291, CA059897.

**Table 1:** Alignment metrics between pathology and MRI

Fixing Method	Global Alignment Overlap	Line-by-line Alignment Overlap	Dist. b/w Landmarks [mm]
<b>Molded [n=5]</b>	$61.7 \pm 8.5\%$	$99.5 \pm 0.51\%*$	Avg= $2.1 \pm 1$ max=6.5
<b>Unmolded [n=5]</b>	$65.8 \pm 12.2\%$	$99.6 \pm 0.55\%*$	Avg= $2.9 \pm 2$ Max=8.0

\* p<0.00001, paired t-test, line by line vs. global